Integral model for multiple forced plumes arranged around a circle in a linearly stratified environment

Zhiguo He [1,2,*] and Yingzhong Lou [1]

[1]*Institute of Port, Coastal, and Offshore Engineering, Ocean College,*
Zhejiang University, Zhoushan 316021, China
[2]*State Key Laboratory of Satellite Ocean Environment Dynamics, Second Institute of Oceanography,*
Ministry of Natural Resources, Hangzhou 310012, China

An integral model is developed to describe the merging of multiple forced plumes released from sources arranged evenly around a circle against a linearly stratified background. The velocity potential of an array of line sinks is introduced to identify the distorted boundaries of interacting plumes. The variation of the entrainment coefficient for forced plumes is modeled as a function of the local Richardson number in the model and an improved entrainment assumption based on the boundary-curvature analysis is proposed to regulate the merging. The present model is shown to be feasible to provide a self-consistent prediction for the dynamics of multiple coalescing forced plumes. The amplification of the maximum rise height of two plumes due to superposition is faithfully reproduced and its scaling predicted by the model is reasonably consistent with the observations of available experiments. The model results further suggest that the mean entrainment efficiency per unit length of the plume boundary attains a local minimum at the touching height, implying significant mutual entrainment in that region.

I. INTRODUCTION

The process of multiple forced plumes abounds in both the natural environment and human activities. For instance, it plays an important role both in the upwelling flows formed by the discharge of meltwater at the base of glaciers [1–3] and in the hydrothermal fluids issued from a cluster of submarine black smoker vents around an ocean ridge [4–6]. Meanwhile, the interaction of multiple plumes is also relevant to the discharging of treated wastewater from coastal cities via submarine outfalls [7,8], the air circulation generated by multiple heat sources in naturally ventilated spaces [9,10], and the design optimization of an array of cooling towers [11,12].

Several experiments have been conducted to investigate the propagation of multiple plumes [13–19], and these observations have provided valuable guidance for general theories. Specifically, Baines and Keffer [20] obtained the velocity profiles and turbulence characteristics of multiple jets with a series of experiments at ambient temperature, which may shed light on the development of clouds and the generation of heat island effects. Brahimi and Doan-Kim-Son [21] reported an experiment on the interaction of two equal turbulent plumes generated by a heated copper disk; they observed a development region between the height where the plumes begin to interact and the height where the plumes are no longer distinguishable. Most recently, He *et al.* [22] made a detailed study of turbulent forced plume pairs with different separations in a stratified environment using the

---

*Corresponding author: hezhiguo@zju.edu.cn

particle image velocimetry technique. Their results provided a reasonable estimate of the maximum penetration scaling for two interacting plumes.

Coalescing plumes have also been simulated using numerical methods [23–25]. In particular, a Lagrangian plume model proposed by Alessandrini *et al.* [26] was used to consider the case of two plumes in a neutral atmosphere, in which an artificial scalar indicating the temperature difference between the plume and the environment was introduced to simulate the entrainment. Zhou *et al.* [27] used a direct numerical simulation approach to investigate the velocity structures of two plane jets with different source separations in uniform coflow; their results suggest that the merging distance may have a linear correlation with the source separation. Lou *et al.* [28] simulated two coalescing turbulent forced plumes in a stratified environment using finite-volume methods, implying that the superposition of two plumes could lead to the distortion of plume boundaries and the entrainment coefficient would decrease in the touching region of two plumes due to mutual entrainment.

Integral models have been developed to describe the dynamics of interacting plumes, as this approach tends to be more economical in computational cost than those numerical simulations. Davidson *et al.* [29] presented an approximate solution to the merging of an infinite array of equally spaced buoyant jets by assuming that the vertical velocities from the individual sources are additive. Kaye and Linden [30] proposed a model for two coalescing pure plumes in an unstratified environment; they modeled the interaction between plume pairs through a shift of the plume axes due to mutual entrainment. Based on the assumption of a constant entrainment coefficient, this model made a prediction of the merging height that shows good agreement with observations. Cenedese and Linden [31] extended that work by introducing the transition region where two plumes touch each other but are not yet merged. Under the same entrainment assumptions, the extended model provided an estimation of the total volume flux that compared favorably with their laboratory experiments in all three regions. It should be noted that a merging height scaling that is significantly larger than the prediction of Kaye and Linden [30] was also reported by Yannopoulos [32], who developed a model containing the effect of superposition to predict the mixing of multiple buoyant jets. Recently, an integral model considering the complex potential of an array of line sinks was proposed by Rooney [33] to predict the merging of an infinite row of plumes or jets in a uniform ambience. This model, in which the plume boundaries were identified with the contours of velocity potential and the entrainment was estimated by the volume flux across the plume boundaries, could provide reasonable limiting similarity solutions near the touching height, i.e., the height where the plumes begin to merge, and derive a touching height scaling for a row of pure plumes which is comparable to that for two equal plumes implied by Kaye and Linden [30]. Furthermore, Rooney [34] presented an extended model to describe the merging of pure or slightly forced plumes whose sources are evenly spaced around a circle. By employing the methods developed by Rooney [33] and closing the governing equations with a modified entrainment assumption, this model was shown to yield the evolution of plume volume flux which agrees well with that observed in the experiments in a homogeneous environment.

However, there are very few theoretical studies focusing on the multiple forced plumes in a stratified environment. Hence, our aim is to improve the integral model to be applicable in a linearly stratified ambience for the sake of describing the dynamics of two or more plumes before reaching the maximum rise height and better understanding the physical mechanisms of interacting forced plumes. The theoretical framework considering the variability of both the buoyancy flux and the entrainment coefficient is presented in Sec. II; the governing equations are also described in this section. An application of the present model to the merging of two forced plumes is presented and discussed in Sec. III. Conclusions are summarized in Sec. IV.

II. INTEGRAL MODEL

The present model for multiple forced plumes in a stratified ambience is proposed based on the theory of potential flows. Here we first introduce the framework for modeling the entrainment of interacting plumes by an array of line sinks, as proposed by Kaye and Linden [30] and

Rooney [33,34], and then extend it to close the generalized plume equations in a linearly stratified environment.

A. Potential flow assumptions

The dynamics of coalescing plumes, especially the mean entrainment velocity field and the boundary distortion, in the merging regions may be approximated by line sinks [30], and the velocity potential Ω due to multiple equal line sinks equally spaced around a circle can be given by [34]

$$\Omega = -\frac{m}{2\pi} \ln(Z'^n - 1) - \frac{m}{2\pi} \ln R^n + \Pi, \tag{1}$$

where n is the number of line sinks, $-m(z)$ is the strength of each line sink, R is the radius of the circle, $Z' = x/R + iy/R$ is a dimensionless complex variable, and Π is an arbitrary constant. In the integral model, possible plume boundaries can be identified by the lines to which the local streamline is orthogonal, i.e., the contours of equal velocity potential [34]. According to Eq. (1), since R is a constant in a prescribed case, these contours can be represented as $|Z'^n - 1| = k$, where k is constant. Considering one representative plume sector, taken here as $-\pi/n \leqslant \theta \leqslant \pi/n$, this equation can be further simplified to

$$\rho^{2n} - 2\rho^n \cos n\theta + 1 = k^2 \tag{2}$$

in the polar coordinates (ρ, θ), where $Z' = \rho e^{i\theta}$ [34]. Furthermore, based on the potential flow theory and Eq. (2), the flow speed magnitude q on the contours can be expressed as

$$q = \left|\frac{d\Omega}{dZ}\right| = \frac{1}{R}\left|\frac{d\Omega}{dZ'}\right| = \frac{m}{2\pi R}\sqrt{\frac{n^2 \rho^{2n-2}}{\rho^{2n} - 2\rho^n \cos n\theta + 1}} = \frac{m}{2\pi R}\frac{n\rho^{n-1}}{k}, \tag{3}$$

and hence the entrainment flux for one sector can be obtained by a line integral.

B. Governing equations

The governing equations of a plume sector with top-hat profiles in a stratified environment can be written as [33,35]

$$\frac{d}{dz}(wV) = \frac{B}{w}, \tag{4a}$$

$$\frac{dV}{dz} = E, \tag{4b}$$

$$\frac{dB}{dz} = -VN^2, \tag{4c}$$

where w is the vertical velocity, $B = Awg'$ and $V = Aw$ are the buoyancy flux and the volume flux, respectively, $E = \int_C q\, ds = m$ is the entrainment volume flux per unit height across the plume-ambient boundary C, ds is the line element [34], A is the sector area enclosed by an open or closed contour [34], g' is the reduced gravity, and N is the background buoyancy frequency. Since the buoyancy frequency is a nonzero constant in a stably stratified environment with a uniform density gradient, the buoyancy flux in each plume sector is not conserved.

Considering that the variability of the entrainment coefficient has been observed in transitional flow regimes including forced plumes [36–38], a modified entrainment assumption is introduced to close equations (4) and can be expressed, according to Eq. (3), as

$$E = m = q_e R f_e = f_r \alpha w R f_e, \tag{5}$$

where q_e is the local maximum flow speed magnitude attained at the maximum radial extent of each contour, i.e., on the symmetry axis $\theta = 0$ [34], α is the entrainment coefficient for the forced plumes with top-hat profiles and will be described below, f_r is a modification coefficient introduced

to parametrize the effects of boundary distortion and will be defined below, and f_e is a parameter consisting of all dimensionless quantities and can be expressed as [34]

$$f_e = \frac{2\pi k}{n(k+1)^{(n-1)/n}}. \tag{6}$$

It should be noted that, although Eq. (5) is similar in form to Rooney's assumption [34], the present modification is considered as a general extension of the classic entrainment assumption proposed by Morton *et al.* [35] rather than the layering of hypotheses. Meanwhile, these functions are mainly based on the potential flow theory and the analysis of boundary curvature, and their feasibility will be assessed further below.

In the present model, α would not be involved in the nondimensionalization as it is not assumed to be constant. Using $B_0^{1/4}N^{-3/4}$, with $B_0 = B(0)$ the source buoyancy flux, and N^{-1} to obtain dimensionless length and time, respectively, the dimensionless variables denoted by an overbar are given by

$$\bar{w} = \frac{w}{B_0^{1/4}N^{1/4}}, \tag{7a}$$

$$\bar{V} = \frac{V}{B_0^{3/4}N^{-5/4}}, \tag{7b}$$

$$\bar{B} = \frac{B}{B_0} \tag{7c}$$

and

$$\bar{z} = \frac{z}{B_0^{1/4}N^{-3/4}}, \tag{7d}$$

$$\bar{R} = \frac{R}{B_0^{1/4}N^{-3/4}}. \tag{7e}$$

Therefore, the dimensionless governing equations for a plume sector with top-hat profiles in a linearly stratified environment can be obtained as

$$\frac{d\bar{w}}{d\bar{z}} = \frac{\bar{B}}{\bar{w}\bar{V}} - \frac{\bar{w}^2\bar{R}}{\bar{V}}\alpha f_e f_r, \tag{8a}$$

$$\frac{d\bar{V}}{d\bar{z}} = \alpha\bar{w}\bar{R}f_e f_r, \tag{8b}$$

$$\frac{d\bar{B}}{d\bar{z}} = -\bar{V} \tag{8c}$$

and the dimensionless area covered by a plume sector can be defined as

$$A' = \frac{A}{R^2} = \frac{V/w}{R^2} = \frac{\bar{V}}{\bar{w}\bar{R}^2}. \tag{9}$$

C. Forced plume entrainment

Since the entrainment in plumes has been widely observed to be larger than that in jets [39,40] and this phenomenon is considered to be due to the turbulence induced by buoyancy [38,41], the entrainment coefficient of forced plumes with top-hat profiles may be empirically modeled as [42]

$$\alpha = \alpha_j \exp\left[\ln\left(\frac{\alpha_p}{\alpha_j}\right)\left(\frac{\text{Ri}}{\text{Ri}_p}\right)^2\right], \tag{10}$$

where $\alpha_j = 0.075\,66$ and $\alpha_p = 0.1178$ are the entrainment coefficients for jets and pure plumes with top-hat profiles, respectively [36,43], and Ri is the local Richardson number defined in the present study as [36,42,44]

$$\mathrm{Ri} = \frac{V B^{1/2}}{M^{5/4}} = (\mathrm{sgn}\bar{B})|\bar{B}|^{1/2}\bar{V}^{-1/4}\bar{w}^{-5/4}, \tag{11}$$

where $M = Vw$ is the momentum flux and $\mathrm{sgn}\bar{B} = \pm 1$ is the sign function. In particular, Ri_p is the plume Richardson number considered to be constant with a value of 0.557 in the present model [42]. Furthermore, by treating the fountainlike flow as a momentum-driven jet, the entrainment coefficient above the neutrally buoyant layer may be assumed to be a constant, i.e., α_j [45,46].

It should be noted that when plumes touch each other, i.e., $k > 1$, the local Richardson number for the merged plume may be expressed as [34]

$$\mathrm{Ri}_t(z) = \frac{(nV)(nB)^{1/2}}{(nM)^{5/4}} = n^{1/4}\mathrm{Ri}(z). \tag{12}$$

Therefore, in order to avoid the discontinuity at the touching height, the trajectory of the local Richardson number in the present model is approximated by a logistic function of k [47]. Specifically, a modified Richardson number $\mathrm{Ri}_m(z)$ is introduced to smooth the transition and is defined as

$$\mathrm{Ri}_m(z) = \left[\frac{n^{1/4} - 1}{1 + e^{-S(k-1)}} + 1\right]\mathrm{Ri}(z) \rightarrow \begin{cases} \mathrm{Ri}_t(z), & k \gg 1 \\ \mathrm{Ri}(z), & k \ll 1, \end{cases} \tag{13}$$

where S is the steepness of the logistic curve and is taken here as 10. In addition, the values of the local Richardson number and the corresponding entrainment coefficient for the initial condition are denoted by Ri_0 and α_0, respectively.

D. Merging entrainment

The governing equations of plumes in a stratified environment, i.e., Eqs. (8), can be integrated numerically from the source to the maximum plume rise height $\bar{z}_{\max}$ in combination with appropriate initial conditions and a feasible entrainment assumption. In particular, the parametrization of f_r used in the present model is discussed in the following.

In nonsimple flow regimes (e.g., the transition from jets to plumes, and the touching regions of multiple plumes), the entrainment coefficient has been reported to be considered variable [34,37,38,48], while its physical mechanisms remain areas of active research [41,49–51]. A relatively simple entrainment assumption, e.g., a constant coefficient, has been shown to be feasible for providing a robust framework for the merging of multiple plumes [30,31,33,34]. Such an assumption, however, may pose a potential risk of underestimating the entrainment when plume interactions are significant [34], since the mutual entrainment will lead to an asymmetry that entrainment velocities generated by different sinks may reinforce each other or cancel each other out.

Partly because of the lack of detailed observations, the understanding of plume behavior in the touching region yet may not be sufficient to effectively guide the parametrization of the entrainment in models allowing for distortion. The existing modifications to the entrainment assumption generally tend to introduce a transitional parameter to scale the entrainment coefficient. For example, Rooney [34] modified the entrainment strength with a well-designed function of the flux-balance parameter $\Gamma_m(z) = \frac{5}{8}n^{1/2}\pi^{-1/2}\alpha^{-1}BV^2M^{-5/2}$ under the assumption of self-regulation. Meanwhile, it is noteworthy that Rooney [33] raised the possibility of regulating the entrainment coefficient by the plume boundary curvature.

In the present model, the effects of the plume boundary curvature on entrainment are analyzed. Specifically, since the relationship between the entrainment velocities at different positions is

known, as Eq. (3) implied, the entrainment flux across any prescribed velocity-potential contour can be uniquely determined by the local q_e [34]. In other words, a modification of the entrainment assumption can be equivalent to regulating the relationship between the mean plume vertical velocity and q_e. Hence, it may be feasible to investigate the boundary curvature on the line of symmetry, i.e., $\theta = 0$, to guide the modification. According to Eq. (2), the curvature at the point $(\rho_{\max}, 0)$ can be obtained as

$$K_0 = \frac{\left| \rho^2 + 2\left(\frac{d\rho}{d\theta}\right)^2 - \rho \frac{d^2\rho}{d\theta^2} \right|}{\left[\rho^2 + \left(\frac{d\rho}{d\theta}\right)^2 \right]^{3/2}} \Bigg|_{\theta=0} = \frac{\left| \rho_{\max}^2 - \rho_{\max} \frac{n\rho_{\max}}{1-\rho_{\max}^n} \right|}{\rho_{\max}^3} = \frac{|k+n|}{k(k+1)^{1/n}}, \tag{14}$$

where $\rho_{\max} = (k+1)^{1/n}$ is the maximum radial extent of each contour [34]. It is worth noting that the entrainment coefficient of a plane plume has been observed to be usually larger than that of an axisymmetric plume [36,52,53]. Based on this observation, it is reasonable to assume that the local entrainment rate is negatively related to a normalized plume boundary curvature $\overline{K}$. Here $\overline{K}$ is defined as the ratio of K_0 to the boundary curvature of a hypothetical plume that is generated by an isolated line sink located at $(1, 0)$ and is tangent to the plume boundary at $(\rho_{\max}, 0)$. Specifically, this parameter can be expressed as

$$\overline{K} = \frac{K_0}{1/(\rho_{\max} - 1)} = K_0[(k+1)^{1/n} - 1]. \tag{15}$$

As expected, $\overline{K}$ decreases first and then increases along with the increase of k and tends to unity in the limits of both small and large k.

The tendency of $\overline{K}$ implies that the entrainment coefficient would increase when plume boundary distortion is significant. However, there is little direct observation that can be used to quantify this effect and then derive an explicit entrainment coefficient. Technically, it is entirely possible to construct a sophisticated function relating the entrainment coefficient to $\overline{K}$. Moreover, the inward shift of the sinks, which was introduced by Kaye and Linden [30], could also potentially be modeled and employed to dynamically modify $\overline{K}$. Such techniques will always be reasonable and effective, but may hardly be regarded as an elegant idea. Instead, as the necessity of the modification is almost certain and the degree of the modification can be estimated by the ratio of the entrainment coefficient of plane plumes to that of axisymmetric plumes, the present model would tend to parametrize f_r using a simple function. Specifically, we can assume that

$$f_r = 2(1 - 1/n)k^2 \exp(-k^2) + 1 \tag{16}$$

since this function can regulate the entrainment according to the tendency indicated by $\overline{K}$ and tends to unity in both of the two limiting cases, i.e., $k \gg 1$ and $k \ll 1$. Such a modified assumption can adequately compensate for the underestimation of the entrainment flux near a circular source due to improper distortion. Moreover, this function attains its maximum at the touching height, where the departure of the shape of plume cross sections from a circle also reaches a maximum. Also, the modification can effectively regulate the entrainment by increasing the estimation of q_e when the distortion is significant and vice versa. Furthermore, the feasibility and effectiveness of this modified assumption will be assessed in the following by comparison with the available experimental observations.

III. MERGING OF FORCED PLUMES IN A STRATIFIED ENVIRONMENT

The two-plume experiments presented by He *et al.* [22] and reproduced by Lou *et al.* [28] through numerical methods are employed to validate the present integral model by discussing the maximum plume rise height as it is one of the most important scalings of the dynamics of plumes in a stratified environment. These experiments involve two forced plumes released from two orifices with a diameter of 7 mm, and the experimental conditions are summarized in Table I. It should be

TABLE I. Summary of the main parameters for the cases employed in both the physical experiments and the present model (SI units). These cases are divided into three groups according to their flow regimes, i.e., the initial Richardson number.

Groups	Cases	$2R$ (m)	N (s^{-1})	B_0 (m^4 s^{-3})	Ri$_0$	k_0
A	1	1.5×10^{-2}	0.90	9.83×10^{-7}	0.421	0.873
A	2	3.0×10^{-2}	0.91	9.93×10^{-7}	0.423	0.461
A	3	6.0×10^{-2}	0.90	9.71×10^{-7}	0.420	0.233
A	4	9.0×10^{-2}	0.89	9.66×10^{-7}	0.417	0.155
A	5	1.2×10^{-1}	0.88	9.73×10^{-7}	0.420	0.117
B	6	1.5×10^{-2}	0.89	1.53×10^{-6}	0.276	0.873
B	7	3.0×10^{-2}	0.87	1.53×10^{-6}	0.275	0.461
B	8	6.0×10^{-2}	0.88	1.53×10^{-6}	0.276	0.233
B	9	9.0×10^{-2}	0.86	1.54×10^{-6}	0.276	0.155
B	10	1.2×10^{-1}	0.87	1.53×10^{-6}	0.276	0.117
C	11	1.5×10^{-2}	0.91	2.40×10^{-6}	0.174	0.873
C	12	3.0×10^{-2}	0.90	2.40×10^{-6}	0.173	0.461
C	13	6.0×10^{-2}	0.89	2.35×10^{-6}	0.172	0.233
C	14	9.0×10^{-2}	0.90	2.41×10^{-6}	0.174	0.155
C	15	1.2×10^{-1}	0.88	2.36×10^{-6}	0.172	0.117

noted that, since the main focuses of the experiments are the interaction between two plumes with different source separations and source buoyancy fluxes in a stratified environment, the buoyancy frequency N is treated as a constant in the experiments. Furthermore, the model behavior is also compared to other theoretical models to investigate the detailed dynamics of coalescing plumes in a stratified environment including neutrally buoyant layers and virtual origins.

The governing equations (8) have been integrated numerically based on these parameters, and 15 single plume counterparts are also modeled for reference. By definition, the dimensionless initial vertical velocity $\bar{w}_0 = \bar{w}(0)$ and volume flux $\bar{V}_0 = \bar{V}(0)$ can be obtained by Eqs. (9) and (11) as

$$\bar{w}_0 = \left(\frac{\bar{B}_0^2}{\text{Ri}_0^4 A_0' \bar{R}^2} \right)^{1/6}, \tag{17a}$$

$$\bar{V}_0 = A_0' \bar{R}^2 \bar{w}_0, \tag{17b}$$

where $A_0' = A'(0)$ and $\bar{B}_0 = \bar{B}(0) = 1$ are initial values of the dimensionless sector area and buoyancy flux, respectively. Meanwhile, since $A_0 = A(0)$ is considered as the cross-sectional area of the orifice, the initial value of k, i.e., k_0, can be recovered accordingly [34], as shown in Table I.

A. Plume dynamics

Focusing on the effect of source separation on plume dynamics, variations of the value of k with $\bar{z}$ for group B, i.e., cases 6–10, are shown in Fig. 1, where the red line indicates the value of 1, i.e., the touching height $\bar{z}_t$. The result suggests that space constraints on plumes will enhance interactions and mixing. Hence, a smaller separation of two sources can lead to a higher growth rate of plume cross-sectional area and an earlier touching.

An illustration of the fully developed two plumes without rebounding for case 7 is given in Fig. 2(a), and the three-plume counterpart is shown in Fig. 2(b) for comparison. The plume boundaries are identified with the velocity-potential contours recovered from the variation of k with $\bar{z}$. Furthermore, several typical contour lines of k are projected onto the plane $\bar{z} = 0$, which indicate the shapes of cross sections of the interacting plumes at different heights.
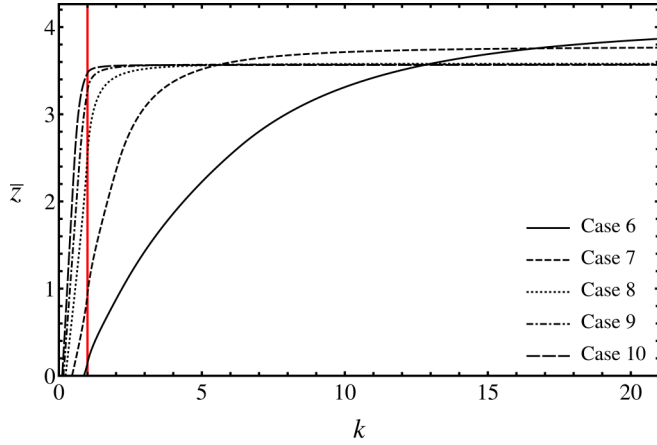
FIG. 1. Solutions for the values of k for cases 6–10. The red line indicates the value of 1, implying the touching height of two plumes.

Figure 3 shows the vertical profiles of $\bar{B}$ for cases 6–10, where the red line indicates the neutrally buoyant plume heights $\bar{z}_{\text{neutral}}$. The mean of those for their single-plume counterparts is also plotted as a blue dashed line for comparison. The solutions suggest that a smaller source separation can generate a lower decay rate of the buoyancy flux. This implies that the touching and merging of multiple plumes may tend to reduce the entrainment of ambient fluid, as a result of significant mutual entrainment.

Variations of dimensionless vertical velocity and momentum along with $\bar{z}$ for cases 6–10 and the mean of those for their single-plume counterparts are shown in Fig. 4. These solutions indicate that the vertical velocity decreases monotonically along with height due to entrainment. Moreover, as expected, the momentum increases first and then decreases along with the increasing height; the turning point in its trajectory is located at $\bar{z}_{\text{neutral}}$, where the buoyancy flux of plumes is zero. In addition, the results suggest that the touching of two plumes will lead to a lower decay rate of the vertical velocity. This further implies that the interaction of two plumes may tend to decrease the entrainment flux of ambient fluid, although the touching will increase the local Richardson number and thus increase the entrainment coefficient.
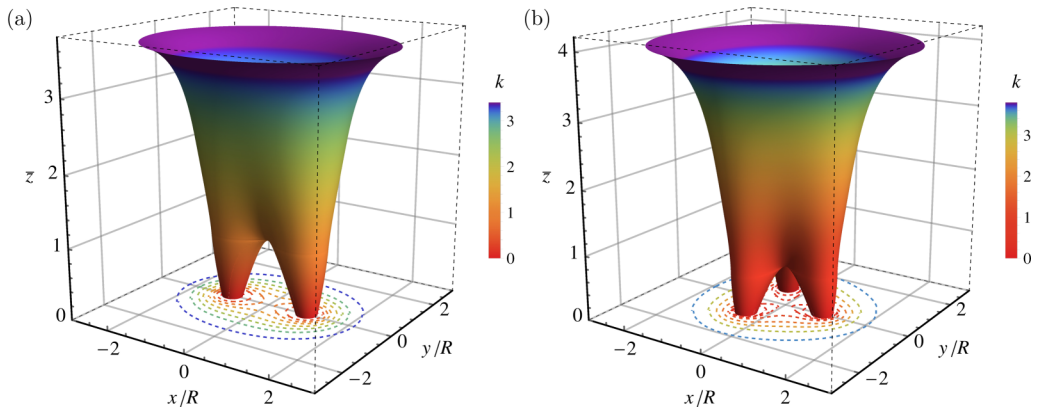

FIG. 2. Illustration of the boundaries of (a) the two plumes for case 7 and (b) the three-plume counterpart. Several typical contour lines of k are plotted and projected onto the plane $\bar{z} = 0$.
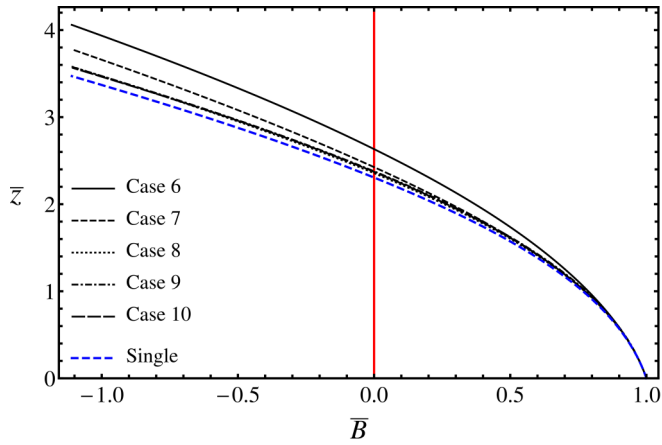
FIG. 3. Solutions for dimensionless buoyancy flux for cases 6–10. The blue dashed line represents the mean of those for the single-plume counterparts and the red line indicates the value of 0, implying the level of neutral buoyancy.
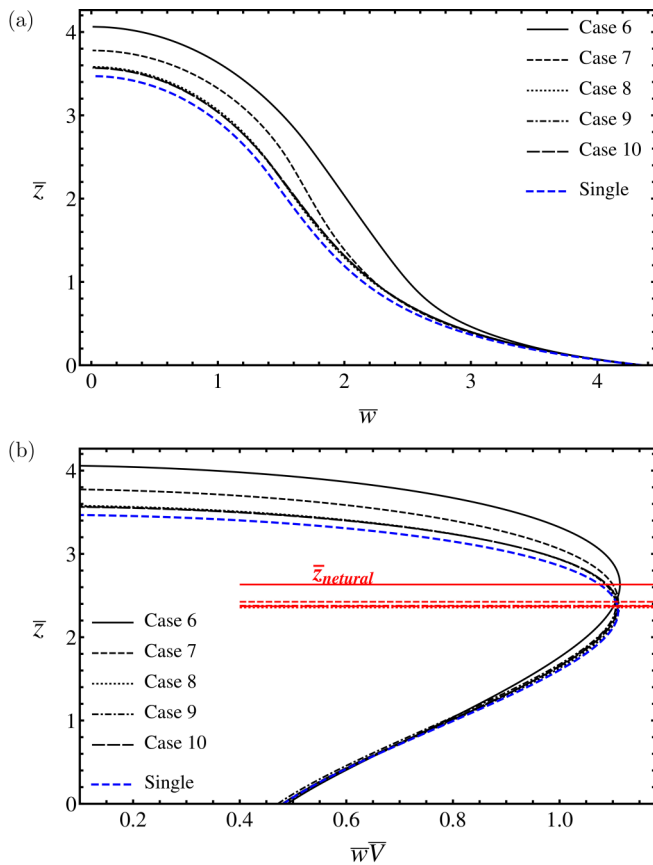

FIG. 4. Solutions for dimensionless (a) vertical velocity and (b) momentum for cases 6–10. The blue dashed lines represent the mean of those for the single-plume counterparts and the horizontal red lines indicate the neutrally buoyant plume heights for each case of two plumes.
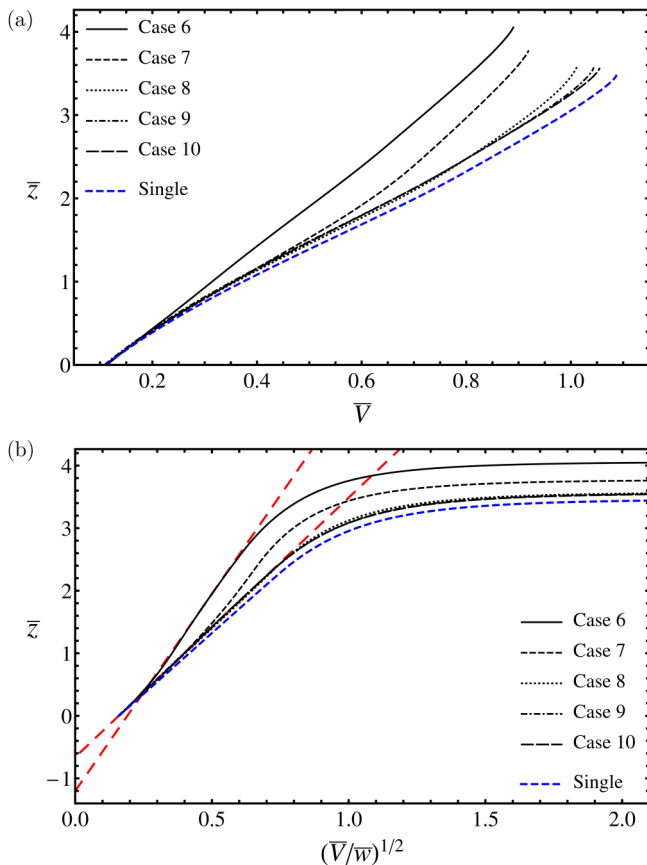
FIG. 5. Solutions for dimensionless (a) volume flux and (b) horizontal plume length scale for cases 6–10. The blue dashed lines represent the mean of those for the single-plume counterparts and the red dashed lines indicate the fitted lines of the horizontal plume length scale in the near vent region and the merging region, respectively.

The variation of both the dimensionless volume flux and horizontal plume length scale, i.e., $(\bar{V}/\bar{w})^{1/2}$, along with $\bar{z}$ for cases 6–10 suggests that there is a significant reduction in plume growth rate at the touching height, as shown in Fig. 5. These tendencies suggest that the mutual entrainment and superposition of plumes can play an important role in the region above the touching height, including producing a decrease in the entrainment of ambient fluid. In addition, the location of the dimensionless virtual origin for an individual plume $\bar{z}_v$ can be calculated by fitting the trajectory of $(\bar{V}/\bar{w})^{1/2}$ in the near source field (taken here as $0 \leqslant \bar{z} \leqslant 0.2\bar{z}_{\max}$) for cases 8–10 and extrapolating back to the height where the plume "radius" is zero. Similarly, the location of the virtual origin for the merged plume $\bar{z}_{vm}$ may be estimated by fitting a straight line for the data of case 6 in the region between the touching height and $\bar{z}_{\text{neutral}}$ (taken here as $0.4\bar{z}_{\max} \leqslant \bar{z} \leqslant 0.5\bar{z}_{\max}$). As shown in Fig. 5(b), the relationship between those two locations implied by the model can be expressed as $\bar{z}_{vm} = \bar{z}_v - 0.234\bar{R}/\alpha_0$, which compares favorably with that predicted by Kaye and Linden [30], i.e., $\bar{z}_{vm} \approx \bar{z}_v - 0.248\bar{R}/\alpha_0$.

B. Maximum plume rise height scaling

All values of $\bar{z}_{\max}$ and $\bar{z}_{\text{neutral}}$ for the two plumes and the single-plume counterparts estimated by the model are summarized in Table II. These scalings predicted by the single-forced-plume theory

TABLE II. Summary of the maximum plume rise heights and the neutrally buoyant plume heights for all two-plume cases and the single-plume counterparts; the predictions of Morton's theory are also listed for comparison.

| Cases	Two-plume case (present model)			Single-plume counterparts (present model)			Single-plume counterparts (Morton's theory)		
	$\bar{z}_{max}$	$\bar{z}_{neutral}$	$\bar{z}_{neutral}/\bar{z}_{max}$	$\bar{z}_{max}$	$\bar{z}_{neutral}$	$\bar{z}_{neutral}/\bar{z}_{max}$	$\bar{z}_{max}$	$\bar{z}_{neutral}$	$\bar{z}_{neutral}/\bar{z}_{max}$
1	3.986	2.621	0.658	3.424	2.310	0.675	3.403	2.342	0.688
2	3.668	2.402	0.655	3.420	2.307	0.674	3.397	2.336	0.688
3	3.529	2.368	0.671	3.422	2.307	0.674	3.401	2.338	0.688
4	3.526	2.380	0.675	3.426	2.311	0.675	3.410	2.345	0.688
5	3.537	2.390	0.676	3.433	2.320	0.676	3.417	2.355	0.689
6	4.063	2.632	0.648	3.463	2.295	0.663	3.532	2.360	0.668
7	3.779	2.425	0.642	3.473	2.307	0.664	3.548	2.377	0.670
8	3.582	2.356	0.658	3.468	2.301	0.664	3.540	2.368	0.669
9	3.574	2.378	0.665	3.480	2.317	0.666	3.559	2.390	0.672
10	3.568	2.371	0.665	3.473	2.308	0.665	3.548	2.378	0.670
11	4.084	2.516	0.616	3.471	2.189	0.631	3.519	2.217	0.630
12	3.819	2.316	0.607	3.475	2.194	0.631	3.525	2.224	0.631
13	3.600	2.240	0.622	3.476	2.191	0.630	3.525	2.221	0.630
14	3.564	2.247	0.631	3.476	2.196	0.632	3.526	2.226	0.631
15	3.568	2.256	0.632	3.481	2.202	0.633	3.535	2.235	0.632
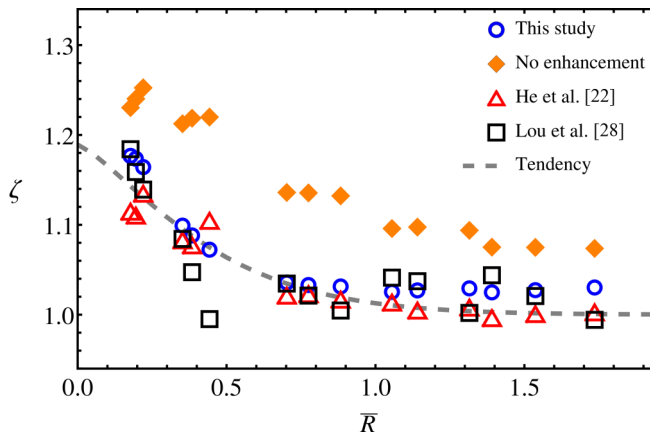
FIG. 6. Comparison between experimental measurements, numerical results, and model predictions for the maximum plume rise height scalings of two plumes with different dimensionless source separations, where the dashed line indicates the tendency of all these data. The outcomes of the present model without any entrainment enhancements, i.e., $f_r = 1$, are also shown for comparison.

[54], in which the entrainment coefficient is chosen as α_0 and the ratio between the length scale for the profiles of buoyancy and that of velocity λ is taken as 1, are also listed for comparison. It is shown that the model results for both the single-plume counterparts and the two plumes with a large source separation agree well with the theoretical predictions.

Meanwhile, the results indicate that the maximum plume rise height may increase by more than 10% due to mutual entrainment when the source separation is sufficiently small; this phenomenon has also been reported in both laboratory experiments [22] and numerical simulations [28]. A framework to evaluate the strong correlation between the maximum plume rise height and the source separation of two plumes has been proposed by He *et al.* [22]. Specifically, they introduced an amplification coefficient ζ as the ratio of the maximum plume rise height for two plumes to that for their single-plume counterpart. Following the definition, the values of ζ for all the cases are shown in Fig. 6.

The comparison of those amplification coefficients suggests that the predictions of the present model are in reasonable agreement with both the experimental observations and the numerical results. In particular, the comparison of the results of the merging-plume model without any entrainment enhancements, i.e., $f_r = 1$, with the experimental data showed that the available forced-plume entrainment assumption may be prone to omit the mutual entrainment between two plumes and thus underestimate the entrainment of distorted plumes. It should be noted that such a difference can hardly be regarded as the divergence between the initial and final rise heights. This is not only because the inconsistency between those predictions and the theoretical upper bound (i.e., the theoretical value of the upper bound is $\sqrt[4]{2} \approx 1.19$ when two plumes are initially merged) is far beyond the range of model uncertainty, but also because, as shown by Bloomfield and Kerr [45], the effect of omitting the interaction between the upflow and downflow could be largely offset by that of neglecting the variation of the environment density at the same time. In this sense, the robustness and practicability of the modified entrainment assumption could be considered satisfactory. Moreover, it should be noted that the present model may tend to slightly overestimate the effects of plume interactions, especially compared with the laboratory results. Although the numerical outcomes imply that such a difference may be in the ranges of experimental and model uncertainties, the discrepancy can be partly explained by the omission of the rebounding flow and the simplifications of the circulation in the plume cap regions in the model.

Specifically, it can be seen that the present model tends to underestimate the maximum rise height for two plumes and their single-plume counterparts compared with the experimental observations
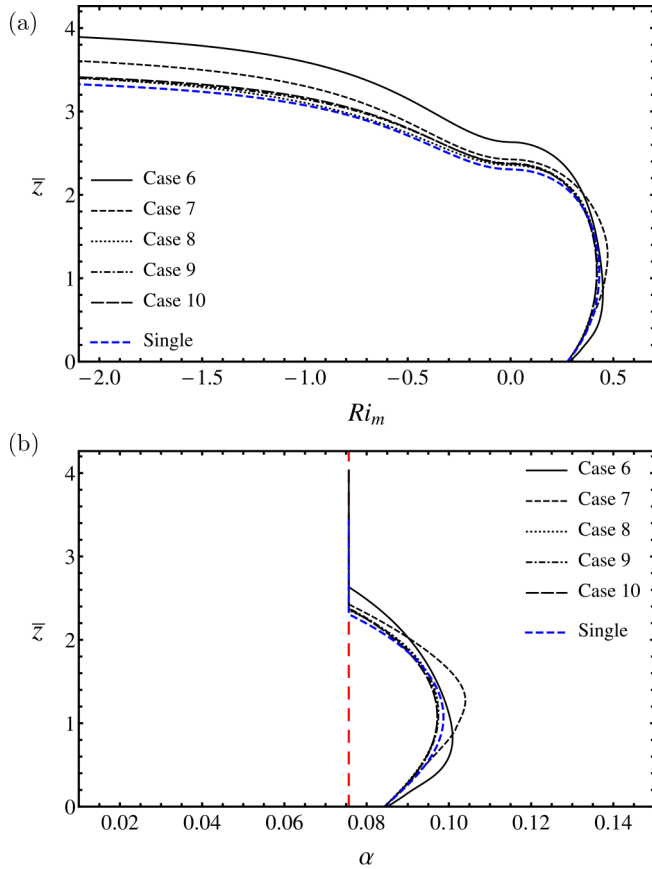
FIG. 7. Vertical profiles of (a) the local Richardson number and (b) the corresponding entrainment coefficient for cases 6–10. The blue dashed lines represent the mean of those for the single-plume counterparts and the red dashed line indicates the value of the entrainment coefficient for pure jets.

[22]. This tendency may be partly due to the omission of the rebound after overshooting, since the counterflow will allow the upflowing plumes to mix with the denser falling fluid instead of the lighter environment. In addition, it is noteworthy that the rebounding flow can also produce the circulation in the plume cap region and the lateral spreading in the neutrally buoyant layer, and both of these effects tend to decrease entrainment of ambient fluid. Hence, as the superposition of multiple plumes will suppress the rebound in the inner region of plume arrays, the model predictions for the two plumes with a smaller source separation may be in better agreement with the observations, thus leading to the overestimation of the amplification coefficient. Moreover, as a result of the omission of the circulation in the plume cap region, the slight distortion of plume sectors near the maximum plume rise height may be non-negligible for those cases with a large source separation [see also Figs. 1 and 5(b)]. Such inherent deformation can decrease entrainment, therefore leading to a slight (∼3%) overestimation of the maximum plume rise height for two plumes compared with that for their single-plume counterparts.

C. Entrainment coefficient

The evolution of the modified Richardson number Ri_m and the corresponding entrainment coefficient for cases 6–10 are shown in Fig. 7. Both of these parameters increase first and then decrease below the neutrally buoyant height. The first increase period is mainly due to the rapid
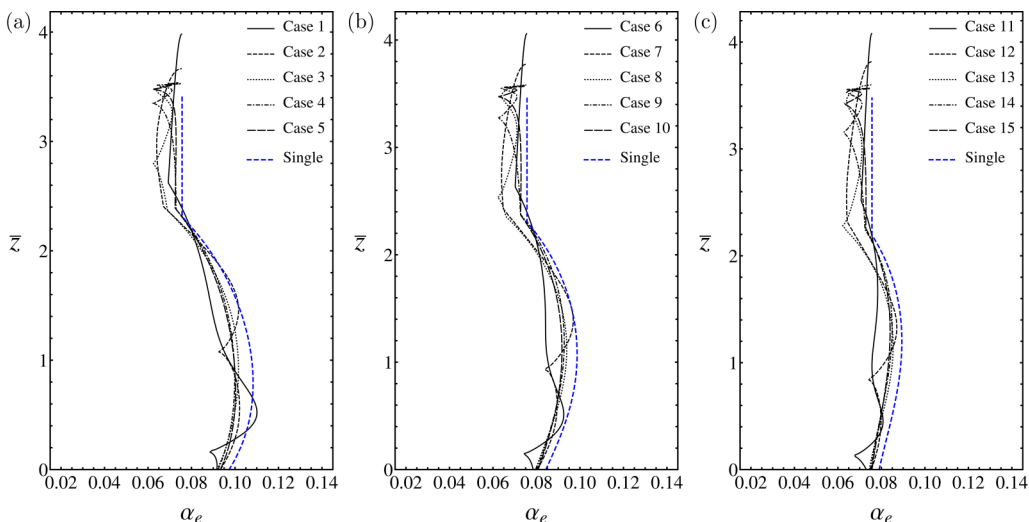
FIG. 8. Vertical profiles of the mean entrainment coefficient for (a) cases 1–5, (b) cases 6–10, and (c) cases 11–15. The blue dashed lines represent the mean of those for the single-plume counterparts.

decay of initial vertical velocity in the near source region, as shown in Fig. 4(a). Meanwhile, the subsequent decrease is largely the result of the continuing decrease of buoyancy flux in a stratified environment. In addition, there is a noticeable shift in the tendency of Ri_m at $\bar{z}_{neutral}$, which is due to the fact that the transition of the flow regime to the forced jets occurs at that level.

Furthermore, a mean entrainment coefficient α_e can be defined to relate the distortion to the total entrainment flux across the boundary of a plume sector. Specifically, according to the entrainment assumption proposed by Morton *et al.* [35], α_e is defined as the mean entrainment efficiency per unit length of plume boundary and obtained by the conservation equation of volume as

$$\alpha_e = \frac{dV}{dz}\frac{1}{wP} = \frac{d\bar{V}}{d\bar{z}}\frac{1}{\bar{w}\bar{R}P'}, \tag{18}$$

where $P = RP'$ is the perimeter of the plume-ambient boundary in one sector and can be expressed as

$$\frac{P}{R} = P' = \int_C ds' = k\int_{-\pi/n}^{\pi/n} \frac{[\cos n\theta \pm (k^2 - \sin^2 n\theta)^{1/2}]^{1/n}}{(k^2 - \sin^2 n\theta)^{1/2}}d\theta \tag{19}$$

for $k > 1$ and

$$P' = 4k\int_{(1-k)^{1/n}}^{(1+k)^{1/n}} \frac{\rho^n}{[4\rho^{2n} - (\rho^{2n} + 1 - k^2)^2]^{1/2}}d\rho \tag{20}$$

for $k \leqslant 1$, where $ds' = \sqrt{d\rho^2 + \rho^2 d\theta^2}$ is the dimensionless line element.

The vertical profiles of α_e for the cases of two plumes are provided in Fig. 8. The results suggest that a considerable spatial change of the mean entrainment efficiency can be observed when the source separation of two plumes is relatively small, while there are only minor differences, i.e., around 5%–10%, between the mean entrainment process of two distantly separated plumes and that of their single-plume counterpart. This phenomenon implies that the variation of amplification coefficients may have the same tendency; this prediction compares well with the results shown in Fig. 6.

Furthermore, it is worth noting that there is a cusp at the touching height, which suggests that the mean entrainment efficiency per unit length of plume boundary attains a local minimum in
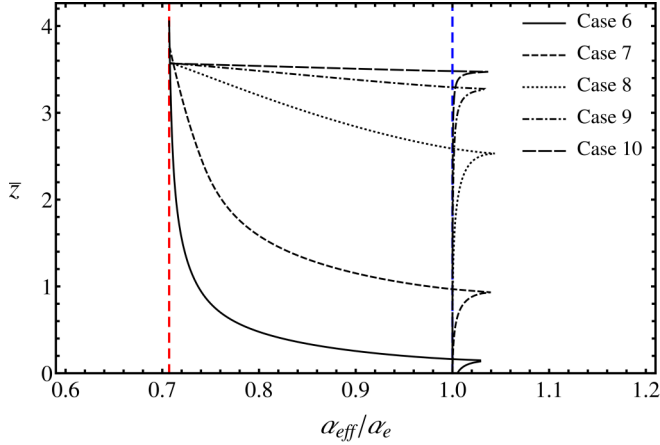
FIG. 9. Dependence of the effective entrainment $\alpha_{\text{eff}}/\alpha_e$ for cases 6–10 with height. The red and blue dashed lines represent the values of $2^{-1/2}$ and 1, respectively.

the regions with significant distortion. This phenomenon can be partly explained by the fact that, according to the potential flow assumption, the superposition will directly lead to distortion of the velocity-potential contours of the plumes with top-hat profiles or an asymmetric horizontal decay rate of the vertical velocity of the plumes originally with Gaussian profiles [28]. Meanwhile, such distortion will affect the distributions of both the entrainment velocity and the curvature of plume boundaries, thus potentially leading to a decrease in the average efficiency of entrainment. In this sense, the lower entrainment rate observed at the touching height could be interpreted as the reduced total entrainment of ambient fluid because of the mutual entrainment accompanying the superposition.

Essentially, the existence of the cusp is a natural consequence of the method employed to identify the plume-ambient boundary, though this turning point may actually imply a transition of the growth behavior of plumes. Specifically, the potential flow assumption employed in the present model determines that the perimeter of a plume sector will show a three-phase variation, i.e., increase, decrease, and increase, with the increase of k. Meanwhile, the first critical point of the nonmonotonic variation is located at the touching height, thus leading to a singularity of the derivative. On the other hand, it can be seen from Fig. 2 that the major growth pattern of plume sectors may change from an inward stretch to a spanwise expansion after touching. In this sense, the cusp may further imply that the merging may replace the deflection as the main dynamic characteristics of two plumes above the touching height.

It should be noted that the lack of continuity of the derivative remains a potential area for improvement. However, the cusp can be smoothed but may not easily be removed by a simple regulator, especially when the support of experimental data is largely absent. In this sense, the existence of the cusp may also imply that the entrainment rate in the touching region may need to be described by a more sophisticated assumption when considering the effect of distortion.

In addition, the effective entrainment coefficient α_{eff} introduced by Cenedese and Linden [31] is investigated to further discuss the effects of touching on the entrainment efficiency. This parameter represents the entrainment needed for several insulated plumes to achieve the same volume and momentum flux as those of the interacting plumes having the same number of sectors. Specifically, α_{eff} can be expressed as

$$\alpha_{\text{eff}} = \frac{1}{2\pi^{1/2}} \frac{dV}{dz} \frac{1}{wA^{1/2}} = \frac{1}{2\pi^{1/2}} \frac{d\bar{V}}{d\bar{z}} \bar{w}^{-1/2} \bar{V}^{-1/2}. \tag{21}$$

The behaviors of α_{eff} for cases 6–10 are shown in Fig. 9. The results indicate that $\alpha_{\text{eff}}/\alpha_e$ first increases, then decreases, and finally tends to the theoretical limit value ($2^{-1/2}$). As the entrainment

coefficient for axisymmetric pure plumes can be regarded as a constant which is independent of plume spatial scalings [55], the tendency suggests that the coalescing plumes would entrain more ambient fluid if they were widely separated. Moreover, it is worth noting that $\alpha_{\text{eff}}/\alpha_e$ reaches its maximum at the touching height, and the nonmonotonicity of a plume perimeter also leads to a singularity of the derivative here. Additionally, the phenomenon that the maximum value of $\alpha_{\text{eff}}/\alpha_e$ is larger than 1 is mainly due to the boundary distortion. Specifically, it is a result of the fact that the perimeter of a distorted cross section will always be larger than that of an axisymmetric one with the same area.

IV. CONCLUSION

An integral model has been proposed to provide a feasible prediction for the mixing of multiple forced plumes arranged around a circle in a linearly stratified environment. Based on the potential flow theory, the model describes the propagation of multiple plumes with top-hat profiles from the source to the maximum plume rise height and yields reasonable dynamic behavior of both the independent and merged plumes.

The superposition of plumes was considered as the primary mechanism of plume interactions in the present model, and the plume boundaries were identified by the contours of the velocity potential due to line sinks. The entrainment coefficient employed in the model was considered as a function of the local Richardson number. Further, a revised merging entrainment assumption based on the boundary-curvature analysis was proposed to regulate the merging. All these approximations have been shown to work well.

The behaviors of the plume boundary distortion, buoyancy flux, vertical velocity, and volume flux derived from the present model are all self-consistent, and all of these dynamic properties suggest that the touching and merging of multiple plumes tend to decrease the entrainment of ambient fluid. The model also provides an estimation of the location of the virtual source for the resulting merged plume, and the prediction is comparable to the available theoretical results. The scaling of the amplification of the maximum rise height in two-plume cases predicted by the model is in reasonable agreement with the available observations. It was also shown that the model tends to slightly overestimate this scaling, though the discrepancy may be partly explained by the omission of both the rebound flow and the circulation in the plume cap region.

The vertical profiles of the mean entrainment coefficient indicate that the mean entrainment efficiency per unit length of plume boundary will attain a local minimum around the touching height, implying that the superposition and the accompanying mutual entrainment will lead to a decrease in the entrainment of ambient fluid. It is worth noting that the temporary decrease of the plume perimeter after touching may result in a singularity of the derivative of the mean entrainment coefficient at the touching height. This implies that a more sophisticated entrainment assumption may need to be considered to describe the plume behavior in the merging region.

---

[1] S. Kimura, P. R. Holland, A. Jenkins, and M. Piggott, The effect of meltwater plumes on the melting of a vertical glacier face, J. Phys. Oceanogr. **44**, 3099 (2014).

[2] D. A. Slater, P. W. Nienow, T. R. Cowton, D. N. Goldberg, and A. J. Sole, Effect of near-terminus subglacial hydrology on tidewater glacier submarine melt rates, Geophys. Res. Lett. **42**, 2861 (2015).

[3] C. Cenedese and V. M. Gatto, Impact of two plumes' interaction on submarine melting of tidewater glaciers: A laboratory study, J. Phys. Oceanogr. **46**, 361 (2016).

[4] K. G. Speer and P. A. Rona, A model of an atlantic and pacific hydrothermal plume, J. Geophys. Res.: Oceans **94**, 6213 (1989).

[5] M. J. Mottl, J. S. Seewald, C. G. Wheat, M. K. Tivey, P. J. Michael, G. Proskurowski, T. M. McCollom, E. Reeves, J. Sharkey, C.-F. You, L.-H. Chan, and T. Pichler, Chemistry of hot springs along the Eastern Lau Spreading Center, Geochim. Cosmochim. Acta **75**, 1013 (2011).

[6] E. T. Baker, Hydrothermal plumes, in *Encyclopedia of Marine Geosciences*, edited by J. Harff, M. Meschede, S. Petersen, and J. Thiede (Springer, Dordrecht, 2016), pp. 335–339.

[7] A. C. H. Lai and J. H. W. Lee, Dynamic interaction of multiple buoyant jets, J. Fluid Mech. **708**, 539 (2012).

[8] J. H. W. Lee, Mixing of multiple buoyant jets, J. Hydraul. Eng. **138**, 1008 (2012).

[9] P. F. Linden, G. F. Lane-Serff, and D. A. Smeed, Emptying filling boxes: The fluid mechanics of natural ventilation, J. Fluid Mech. **212**, 309 (1990).

[10] P. F. Linden, The fluid mechanics of natural ventilation, Annu. Rev. Fluid Mech. **31**, 201 (1999).

[11] L. Pera and B. Gebhart, Laminar plume interactions, J. Fluid Mech. **68**, 259 (1975).

[12] S. Li, A. Moradi, B. Vickers, and M. Flynn, Cooling tower plume abatement using a coaxial plume structure, Int. J. Heat Mass Transfer **120**, 178 (2018).

[13] B. Gebhart, H. Shaukatullah, and L. Pera, The interaction of unequal laminar plane plumes, Int. J. Heat Mass Transfer **19**, 751 (1976).

[14] W. D. Baines, A technique for the direct measurement of volume flux of a plume, J. Fluid Mech. **132**, 247 (1983).

[15] E. Moses, G. Zocchi, and A. Libchaberii, An experimental study of laminar plumes, J. Fluid Mech. **251**, 581 (1993).

[16] C. Y. Ching, H. J. S. Fernando, L. A. Mofor, and P. A. Davies, Interaction between multiple line plumes: A model study with applications to leads, J. Phys. Oceanogr. **26**, 525 (1996).

[17] R. W. Macdonald, R. K. Strom, and P. R. Slawson, Water flume study of the enhancement of buoyant rise in pairs of merging plumes, Atmos. Environ. **36**, 4603 (2002).

[18] D. Contini and A. Robins, Experiments on the rise and mixing in neutral crossflow of plumes from two identical sources for different wind directions, Atmos. Environ. **38**, 3573 (2004).

[19] H. Yamamoto, C. Cenedese, and C. P. Caulfield, Laboratory experiments on two coalescing axisymmetric turbulent plumes in a rotating fluid, Phys. Fluids **23**, 056601 (2011).

[20] W. D. Baines and J. F. Keffer, Entrainment by a multiple source turbulent jet, Adv. Geophys. **18B**, 289 (1975).

[21] M. Brahimi and Doan-Kim-Son, Interaction between two turbulent plumes in close proximity, Mech. Res. Commun. **12**, 249 (1985).

[22] Z. He, W. Zhang, H. Jiang, L. Zhao, and X. Han, Dynamic interaction and mixing of two turbulent forced plumes in linearly stratified ambience, J. Hydraul. Eng. **144**, 04018072 (2018).

[23] R. B. Bornoff and M. R. Mokhtarzadeh-Dehghan, A numerical study of interacting buoyant cooling-tower plumes, Atmos. Environ. **35**, 589 (2001).

[24] M. R. Mokhtarzadeh-Dehghan, C. S. König, and A. G. Robins, Numerical study of single and two interacting turbulent plumes in atmospheric cross flow, Atmos. Environ. **40**, 3909 (2006).

[25] S. N. Oskouie, Z. Yang, and B. Wang, Study of passive plume mixing due to two line source emission in isotropic turbulence, Phys. Fluids **30**, 075105 (2018).

[26] S. Alessandrini, E. Ferrero, and D. Anfossi, A new Lagrangian method for modeling the buoyant plume rise, Atmos. Environ. **77**, 239 (2013).

[27] Y. Zhou, K. Nagata, Y. Sakai, and T. Watanabe, Dual-plane turbulent jets and their non-Gaussian velocity fluctuations, Phys. Rev. Fluids **3**, 124604 (2018).

[28] Y. Lou, Z. He, H. Jiang, and X. Han, Numerical simulation of two coalescing turbulent forced plumes in linearly stratified fluids, Phys. Fluids **31**, 037111 (2019).

[29] M. J. Davidson, D. A. Papps, and I. R. Wood, The behaviour of merging buoyant jets, in *Recent Research Advances in the Fluid Mechanics of Turbulent Jets and Plumes*, edited by P. A. Davies and M. J. V. Neves, NATO Advanced Studies Institute, Series E: Applied Science (Springer, Dordrecht, 1994), Vol. 255, pp. 465–478.

[30] N. B. Kaye and P. F. Linden, Coalescing axisymmetric turbulent plumes, J. Fluid Mech. **502**, 41 (2004).

[31] C. Cenedese and P. F. Linden, Entrainment in two coalescing axisymmetric turbulent plumes, J. Fluid Mech. **752**, R2 (2014).

[32] P. C. Yannopoulos, Advanced integral model for groups of interacting round turbulent buoyant jets, Environ. Fluid Mech. **10**, 415 (2010).

[33] G. G. Rooney, Merging of a row of plumes or jets with an application to plume rise in a channel, J. Fluid Mech. **771**, R1 (2015).

[34] G. G. Rooney, Merging of two or more plumes arranged around a circle, J. Fluid Mech. **796**, 712 (2016).

[35] B. R. Morton, G. Taylor, and J. S. Turner, Turbulent gravitational convection from maintained and instantaneous sources, Proc. R. Soc. London Ser. A **234**, 1 (1956).

[36] E. J. List, Mechanics of turbulent buoyant jets and plumes, in *Turbulent Buoyant Jets and Plumes*, edited by W. Rodi (Pergamon, Oxford, 1982), Vol. 6, pp. 1–68.

[37] H. Wang and A. W.-K. Law, Second-order integral model for a round turbulent buoyant jet, J. Fluid Mech. **459**, 397 (2002).

[38] G. Carazzo, E. Kaminski, and S. Tait, The route to self-similarity in turbulent jets and plumes, J. Fluid Mech. **547**, 137 (2006).

[39] C. J. Chen and W. Rodi, *Vertical Turbulent Buoyant Jets: A Review of Experimental Data* (Pergamon, Oxford, 1980), Vol. 4.

[40] P. F. Linden, Convection in the environment, in *Perspectives in Fluid Dynamics: A Collective Introduction to Current Research*, edited by G. K. Batchelor, H. K. Moffatt, and M. G. Worster (Cambridge University Press, Cambridge, 2000), pp. 289–345.

[41] E. Kaminski, S. Tait, and G. Carazzo, Turbulent entrainment in jets with arbitrary buoyancy, J. Fluid Mech. **526**, 361 (2005).

[42] H. B. Fischer, E. J. List, R. C. Y. Koh, J. Imberger, and N. H. Brooks, *Mixing in Inland and Coastal Waters* (Academic, New York, 1979).

[43] J. S. Turner, *Buoyancy Effects in Fluids* (Cambridge University Press, Cambridge, 1973).

[44] N. E. Kotsovinos and E. J. List, Plane turbulent buoyant jets. Part 1. Integral properties, J. Fluid Mech. **81**, 25 (1977).

[45] L. J. Bloomfield and R. C. Kerr, Turbulent fountains in a stratified fluid, J. Fluid Mech. **358**, 335 (1998).

[46] G. R. Hunt and A. L. R. Debugne, Forced fountains, J. Fluid Mech. **802**, 437 (2016).

[47] X. Yang, J. Liu, Y. Yang, Q. Qing, and G. Wen, An efficient topology description function method based on modified sigmoid function, Math. Probl. Eng. **2018**, 1 (2018).

[48] A. Matulka, P. López, J. M. Redondo, and A. Tarquis, On the entrainment coefficient in a forced plume: Quantitative effects of source parameter, Nonlinear Process. Geophys. **21**, 269 (2014).

[49] A. Ezzamel, P. Salizzoni, and G. R. Hunt, Dynamical variability of axisymmetric buoyant plumes, J. Fluid Mech. **765**, 576 (2015).

[50] M. van Reeuwijk and J. Craske, Energy-consistent entrainment relations for jets and plumes, J. Fluid Mech. **782**, 333 (2015).

[51] D. Krug, D. Chung, J. Philip, and I. Marusic, Global and local aspects of entrainment in temporal plumes, J. Fluid Mech. **812**, 222 (2017).

[52] S. Paillat and E. Kaminski, Entrainment in plane turbulent pure plumes, J. Fluid Mech. **755**, R2 (2014).

[53] T. S. van den Bremer and G. R. Hunt, Two-dimensional planar plumes and fountains, J. Fluid Mech. **750**, 210 (2014).

[54] B. R. Morton, Forced plumes, J. Fluid Mech. **5**, 151 (1959).

[55] J. S. Turner, Buoyant plumes and thermals, Annu. Rev. Fluid Mech. **1**, 29 (1969).